Wood Sci Technol (2016) 50:715–726
DOI 10.1007/s00226-016-0808-2

ORIGINAL

In situ ESEM observations of spruce wood (*Picea abies* Karst.) during heat treatment

Mauro Bernabei[1] · **Maria Cristina Salvatici**[2]

Received: 5 March 2015 / Published online: 15 March 2016

Abstract An environmental scanning electron microscope (ESEM) equipped with a hot stage was used to investigate how the anatomical features of spruce wood respond to heating in vacuum conditions. The ESEM allowed for continuously observing the swelling, shrinkage, and other deformations of certain anatomical elements during heating. Observations showed that, as the temperature increases, there is a slight initial swelling due to thermal expansion of wood and steam and gas release from the cell wall, up to a threshold of 90–100 °C. Subsequently, the size of the various anatomical elements remained stable up to 200 °C, after which the cell walls withdrew and deformed. There were few significant differences between earlywood and latewood, while the deformation of cell lumen was strongly influenced by the dimension and the arrangement of the walls that surrounded them. None of the observed cracks was directly attributable to the impact of increased heat. Nevertheless, existing intercellular spaces strongly increased in size, arriving to grow up to 300 % of the initial dimension. These results emphasize the importance of sound starting materials to avoid defects in the treated samples.

Introduction

Heat treatment of wood and wood-based products is now a widespread practice. However, the variation of several parameters, such as humidity, pressure, time, chemical treatments (Esteves and Pereira 2009), may change the resulting features of the material.

✉ Mauro Bernabei
bernabei@ivalsa.cnr.it

[1] CNR-IVALSA, Trees and Timber Institute, National Research Council, Via Biasi 75, 38010 S. Michele all'Adige, Trento, TN, Italy

[2] Centro di Microscopie Elettroniche "Laura Bonzi" (Ce.M.E.), ICCOM, National Research Council, Via Madonna del Piano 10, Sesto Fiorentino, Italy

As a general rule, thermally treated wood exhibits greater dimensional stability (Giebeler 1983), higher durability (Davis and Thompson 1964; Kamdem et al. 2002), and darker color (Mitsui 2006), and is more brittle than untreated wood (Kubojima et al. 2000). All of these attributes vary depending on the intensity of the treatment, producing materials particularly suited to outdoor, humid, or wet conditions (Xie et al. 2002; Esteves and Pereira 2009).

Nevertheless, if the heat treatment of wood is carried out incorrectly or the original material is flawed (Esteves and Pereira 2009), this may cause defects in the final product (Bourgois and Guyonnet 1988). Such defects are often found as fractures or micro-fractures (Adewopo and Patterson 2011), which, in deciduous species, follow the pathway of the large parenchymatic rays and/or the ring-porous discontinuity (Boonstra et al. 2006b).

There is an extensive bibliography concerning specific aspects of thermal modification and the properties of thermally modified products (Xie et al. 2002; Esteves and Pereira 2009). However, publications regarding the change in microscopic characteristics of the cellular elements during temperature variation are scarce and often conflicting (Pelaez-Samaniegoa et al. 2014; Bryne et al. 2010; Sehlstedt-Persson et al. 2006; Boonstra et al. 2006a), most likely due to the technical difficulties of conducting this type of research. In fact, it is difficult to use traditional microscopy tools to observe structural cell wall changes as the temperature increases. The observations are usually conducted on the same sample at the end of each stage of heating but in a different visual field (Boonstra et al. 2006a, b; Awoyemi and Jones 2011); as a consequence, the description of anatomical characteristics, even when properly done, may not be representative of the experiment.

The main difficulties of the traditional methods of microscopic analysis are as follows:

- Issues related to the preparation of the specimen. In some cases, softening samples via boiling is not appropriate, since boiling may affect the condition of the wood and hide the effects of the treatment. Likewise, cutting the samples can bend the cells and cause small cracks, which may be difficult to distinguish from those resulting from the treatment. It follows that the scanning electron microscope (SEM), which is traditionally used in these research fields, is not fully appropriate for the continuous and repeated observation of the same sample during heat treatment because the specimen has to be cut, dried, and coated with a conductive metal before observation.
- Difficulties in monitoring of exactly the same cellular walls and elements at different temperature levels. In most cases, the cutting and preparation of the specimens prevent one from recognizing with certainty the exact points that were measured in the previous phases.

All these considerations make traditional microscopy techniques poorly suited for studying the effects of heat treatment on wood.

This work presents the advantageous features of the ESEM in comparison with traditional microscopic techniques for in situ studies of the thermal behavior of wood. In particular, the objective of this study is to describe the behavior of some cellular features of spruce wood during heat treatment through an alternative analytical method. Emphasis is placed on the dynamics that generate defects, such as fractures and micro-fractures, and whether they are directly attributable to the heat treatment or are instead an outcome of poor-quality initial material.

Materials and methods

In order to study the thermal transformation of wood, an "in situ" environmental scanning electron microscope (ESEM) with hot stage was used. A FEI Quanta 200 ESEM equipped with a thermal tungsten gun, a gaseous secondary electron detector (GSED), and a 1000 °C hot stage was used for in situ electron imaging. The instrument was operated at 15 kV acceleration potential and with a working distance of about 10 mm.

An advantage to using ESEM in the "wet" mode is that it is not necessary to make samples conductive. The wood does not need to be dried or coated with metal, thus its original characteristics may be preserved (Turkulin et al. 2005a, b).

A differential pumping system allows the entire ESEM specimen chamber to be maintained at a specific gas pressure. A fully automatic electronic servo system holds this pressure constant between 133.3 (1 torr) and 2666.45 Pa (20 torr).

In the ESEM, the vacuum system is divided into multiple stages of increasing vacuum and separated by pressure limiting apertures. There is a differential pumping system that allows the transfer of the electron beam from the high vacuum area in the gun area to the high pressure and low vacuum area in the specimen chamber.

The presence of gas around a specimen, in this case simply water vapor, creates new possibilities that are unique to ESEM, as the gas is electrically conductive and thus prevents negative charge accumulation. The good conductivity of the gas is due to the ionization that undergoes from the incident electron beam and the ionizing GSED.

As a result, specimens can be examined more quickly and easily, avoiding complex and time-consuming preparation methods.

The hot chamber consists of an observation chamber that holds a conduction-heated crucible. Because the temperature (in further text: T) is controlled from the outside, the behavior of the anatomical elements during heating can be observed and described in a *continuum*.

Among all species, spruce (*Picea abies* Karst.) was chosen because it is the most widespread and used species in Italy. Furthermore, like most conifers, its wood is quite homogeneous, without vessels and multi-seriate parenchymatic rays. This facilitates the study of deformations and the interpretation of data.

Samples were taken from four different air-seasoned boards and cut by hand with a razor blade to avoid excessive heating of the surfaces due to the use of mechanical instruments. By contrast, hand cutting of unsoftened samples inevitably produced low-quality surfaces for observation. Once the samples were reduced to cubes of about 3 mm (i.e., a useful size for the hot chamber), they were conditioned to a moisture content of 10–12 % and observed on the cross section.

The images were acquired constantly with a magnification of 1200×. The total number of scanned images was 259. *T* was increased from ambient conditions (approximately 23 °C) up to 400 °C in increments of approximately 7 °C/min (Table 1). Images were acquired at the following temperatures: ambient *T*, 100, 150, 170, 190, 210, 230, 250, 270, 290, 310, 330, 350, 370, and 390 °C. The pressure (*P*) conditions within the hot chamber were maintained at the low and constant value of 3.15 mbar. Attempts to increase the pressure inside the chamber using gases other than oxygen (i.e., argon and nitrogen) proved ineffective. Scanning image quality is lower with argon and nitrogen, because the pressure is unstable.

The anatomical elements that were observed and measured on the cross section are (Table 2): latewood tangential (LWT) and radial (LWR) cell wall; earlywood tangential (EWT) and radial (EWR) cell wall; fractures (FR); parenchymatic rays (RAY); earlywood radial (ERL) and tangential (ETL) lumen diameter; and latewood tangential (LTL) and radial lumen diameter (LRL). Some of these elements are shown in Fig. 1. The measurements were performed on digital images, selected according to quality and *T*, using the UTHSCSA ImageTool program (developed at the University of Texas Health Science Center at San Antonio, Texas and available from the Internet by anonymous FTP from maxrad6.uthscsa.edu).

The measurements were all linear. Initial attempts to take measurements based on the number of pixels per image were unsuccessful. To improve accuracy, each measurement was repeated at least 10 times and then averaged.

During this first experimental phase, the pressure was kept constant to reduce the number of variables. *T* was raised continuously and without ramps (long phases at certain states of *T*). With the aim of stabilizing the conditions within the observation chamber, about 2 min were taken prior to each image acquisition.

Table 1 Experimental settings

Instrument	FEI Quanta-200
Temperature	~20–400 °C
Pressure	3.15 mbar
Heating	7 °C/min
Wood moisture content	~10–12 %

Table 2 Average dimensional changes (%) of particular anatomical elements and their features

T (°C)	Duration (min)	Wood-anatomical characteristics									
		LWT	LWR	EWT	EWR	FR	RAY	ERL	ETL	LTL	LRL
100	11	3.7 (0.29)	0.8 (0.25)	−0.2 (0.23)	−1.4 (0.18)	43.3 (0.06)	−4.7 (0.24)	0.7 (0.10)	−0.2 (0.05)	0.7 (0.12)	−0.7 (0.13)
150	20	3.5 (0.18)	−1.7 (0.20)	−0.8 (0.19)	−4.9 (0.23)	37.9 (0.09)	−4.7 (0.15)	−0.7 (0.12)	0.3 (0.08)	−1.1 (0.11)	−2.3 (0.13)
200	29	5.5 (0.30)	5.1 (0.26)	2.4 (0.12)	−2.8 (0.10)	53.8 (0.05)	−7.2 (0.19)	1.6 (0.14)	10.8 (0.13)	1.6 (0.28)	2.1 (0.12)
250	38	0.5 (0.30)	4.4 (0.20)	−9.2 (0.21)	−11.0 (0.16)	80.9 (0.07)	−9.4 (0.23)	6.4 (0.11)	16.6 (0.09)	−4.3 (0.23)	14.4 (0.10)
300	47	−0.6 (0.25)	0.0 (0.21)	−13.6 (0.17)	−18.6 (0.24)	107.5 (0.07)	−20.7 (0.19)	12.0 (0.12)	12.7 (0.07)	−13.4 (0.24)	23.7 (0.11)
350	56	−9.8 (0.20)	−9.4 (0.19)	−11.5 (0.20)	−13.6 (0.23)	198.7 (0.09)	−29.5 (0.15)	8.7 (0.10)	16.1 (0.07)	−20.2 (0.10)	18.3 (0.08)
400	65	−16.8 (0.35)	−10.8 (0.23)	−7.5 (0.16)	−26.5 (0.22)	214.6 (0.07)	−37.1 (0.15)	11.7 (0.26)	33.1 (0.23)	−23.2 (0.34)	16.6 (0.18)

Standard deviation is in brackets. Minutes of heating are cumulative

LWT latewood tangential cell wall thickness, *LWR* latewood radial cell wall thickness, *EWT* earlywood tangential cell wall thickness, *EWR* earlywood radial cell wall thickness, *FR* fracture, *RAY* parenchymatic ray, *ERL* earlywood radial lumen diameter, *ETL* earlywood tangential lumen diameter, *LTL* latewood tangential lumen diameter, *LRL* latewood radial lumen diameter

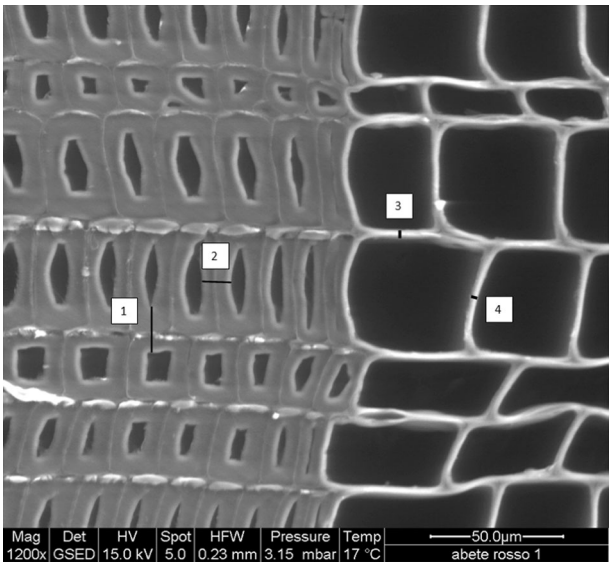

Fig. 1 Some of the elements measured (Table 1). The environmental conditions inside the chamber are shown at the bottom of the picture

Results

The cell wall

The cell wall thickness showed similar nonlinear behavior in all of the analyzed types of cells and their measured elements. In the first phase (up to about 100 °C), the cell wall thickness was characterized by dimensional swelling. Subsequently, approximately between 100 and 200 °C, the dimensions remained almost constant, and temperatures greater than 200 °C induced a rapid reduction in cell wall thickness. At the end of the treatment (about 400 °C), the average reduction in cell wall thickness was above 18 %, with peaks of 39 % (Fig. 2). Analysis of variance showed no significant differences between earlywood and latewood, as regards cell wall thickness ($F = 1.18$, $p > 0.5$) or radial and tangential cell wall thickness.

The cell lumen

The cell lumen size showed contradictory variations with increased T. In general, at the end of the observation, lumen width had decreased by about 10 %; this predominantly occurred in the latewood in the tangential direction. However, some data varied significantly from average result, indicating that the lumen retained comparable dimensions during the entire experiment or in a few cases that it had increased in size (Fig. 5, white circle). The differences between tangential and

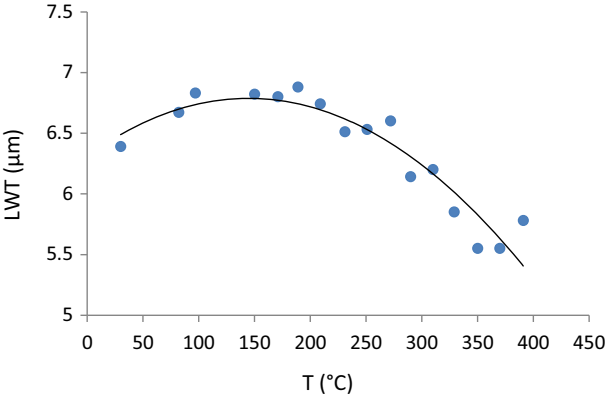

Fig. 2 Variation in the latewood tangential wall (LWT) thickness of sample 2, expressed in absolute terms. The *dots* are fitted with a second-order curve ($r = 0.94$)

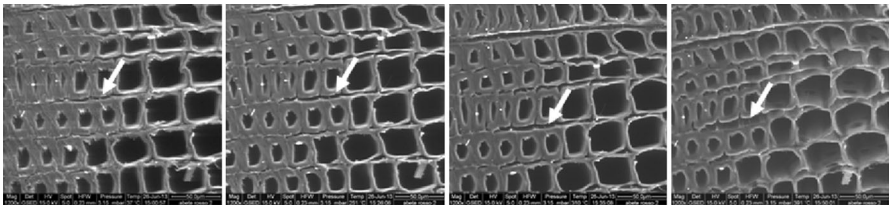

Fig. 3 Sample 2, as observed at 37, 251, 310, and 391 °C, respectively. Note the reduced cell wall thickness and the emphasis of the intercellular spaces (*last picture on the right*), where the sample began to curl in on itself as a result of the temperature

radial ($F = 8.78$, $p < 0.01$) and between earlywood and latewood variations ($F = 3.40$, $p < 0.05$) were significant.

The fractures

Cracks on the cell wall which were directly attributable to the rising T were not observed. By contrast, existing intercellular spaces strongly increased in size (Table 2; Fig. 3).

A slight furrow between the tracheids (i.e., a trace of a parenchymatic ray) widened significantly during the experiment and, by the end of the treatment ($\sim$400 °C), its size had increased by over 300 %.

The parenchymatic rays

The parenchymatic rays were measured along the entire tangential width, including both the walls and the intercellular spaces. In general, by the end of the experiment, the rays had decreased substantially, up to 37 % of their initial size.

Other elements

The observation of other elements during the heat treatment (i.e., the cell walls of the parenchymatic rays, pits chambers, and pits membranes) gave conflicting results: In some cases, the same element swelled up, and in other cases, it shrank with increasing temperature.

Discussion and conclusion

ESEM enabled the observation of the dimensional characteristics of the cellular elements during the entire experiment, thereby supporting the experimental hypothesis. However, some drawbacks should be highlighted:

- In some cases, the images were not as sharp and clear as those obtained with the SEM, resulting in decreased measurement accuracy. This problem was partially dealt with by increasing the number of observations.
- Some images appeared to be deformed by the acquisition system of the instrument. This issue was overcome thanks to the large number of available images, from which the most suitable images were selected.

The cell wall showed a well-defined behavior that was valid for each type of analyzed element. In the first phase of heating, up to about 100 °C, the increase in the width of the wall was probably due to the pressure produced by steam and other gases. In fact, the moisture contained in the samples (approximately 12 %) suddenly started to boil, due to the low pressures inside the chamber (3.15 mbar); the vapor pushed on the walls and membranes that were preventing the outflow and produced the observed swelling of the cell wall. Evidently, other gases, which had been produced in the cell wall during the early stages of the experiment, took part in this phenomenon as well.

An extreme example of this mechanism is seen in sample 1 (Fig. 4). When the sample had reached approximately 90 °C, bubbles began to appear on the sample's

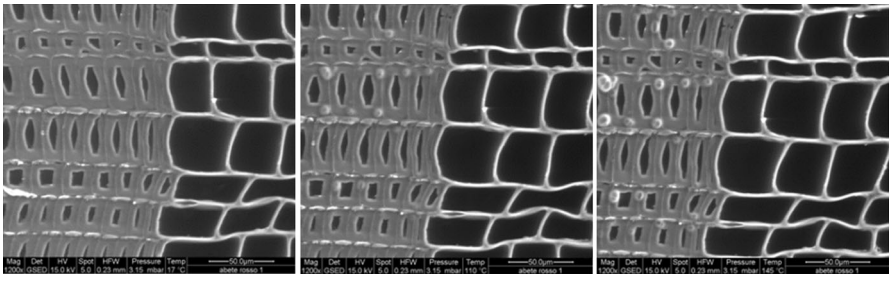

Fig. 4 Sudden escape of vapor from the cell walls produced swelling of bubbles on the cross section of the wood. The same sample is observed at 17, 110, and 145 °C, respectively. When the wood reached 150 °C, the explosion of bubbles knocked the sample out of the strut inside the microscope

cross section. Finding no other plausible explanation, it was hypothesized that the bubbles were caused by the sudden release of steam and other gases from the cell wall, which encountered obstacles to evaporate and instead swelled into blisters, principally in layer S2 of the secondary cell wall. Fengel and Wegener (1989) have already observed this phenomenon, attributing it to melting effects on the surface of cellulose fibers by applying a rapid heating. They also found that similar effects can be produced in a scanning electron microscope if a small area of cellulosic fibers is exposed to a high-energy electron beam.

It is reasonable to assume that the breaking of the blisters can cause fractures in the cell walls, but there is no clear evidence of this. A similar phenomenon was also reported by Xie et al. (2002).

The threshold of 90 °C seems to correspond to prior observations of the thermal softening of wood (Blechschmidt et al. 1986), where a threshold of 115 and 145 °C was identified for conifers (including spruce). The *vacuum* conditions of the environment inside the chamber lowered this threshold.

In all analyzed cases, a marked reduction in cell wall size started only at around 200 °C, confirming the observations of other authors (e.g., Biziks et al. 2013) who used conventional microscopy methods.

The apparent differences between latewood and earlywood, and between radial and tangential cell walls, were not confirmed statistically. The only significant differences were observed in the cell lumen. It is likely that the problems encountered in the use of ESEM (i.e., low-resolution images, deformation) made the measurement results unreliable, especially for smaller items such as the walls of earlywood or pit membranes (see "other elements" paragraph); however, it is also likely that the behavior of the cell wall is not as straightforward as initially assumed. In fact, if analyzed individually, the cellular elements seem to be coherent (Fig. 2), but when the elements are analyzed together, the dispersion of the data greatly increases and the phenomenon is more difficult to interpret. This indicates, therefore, a peculiar behavior of every single element, as a function not only of the characteristics taken into consideration (late/earlywood, radial/tangential direction) but also of other features, such as the size of the wall, its particular chemical composition.

A typical example are the changes in cell lumen size; even if the average decrease at the end of the treatment was approximately 10 %, the variability for individual cells is very high and is affected by the complex system of forces acting on the walls that hold the cell together (Fig. 5, please note the white circle). In

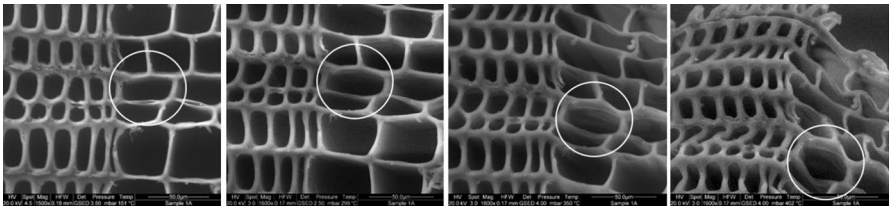

Fig. 5 Increase in T resulted in curling, rotation, and tilt of the sample from the original position. Pictures were taken at 151, 299, 350, and 402 °C, respectively

certain cases, some dimensions may even strongly increase at the end of the treatment, as a result of the forces exerted on the lumen by the surrounding cells.

Another interesting aspect is related to the formation of cracks during heating.

In general, during thermal treatment changes in the chemical composition, components' ratio, and in the wood microstructure, all occur simultaneously (Biziks et al. 2013). Chemical modifications are a complex issue and are not clearly recognizable in microscopic analysis, and therefore, they will not be taken into account in this discussion. Conversely, according to Boonstra et al. (2006a), thermal treatment also affects the anatomical structure of the wood, but the effects depend on the wood species and the process used.

In the current experiment, no cell wall cracks could be directly attributed to the heat treatment. This contrasts with other experimental observations, where the heat treatment of wood resulted in the destruction of tracheid walls and ray tissues (Awoyemi and Jones 2011) or in the separation of fibers and the formation of voids and cracks among them (Biziks et al. 2013).

Perhaps the ESEM technique is not sensitive enough to show the compound middle lamella delamination or S2 layer cracking (Biziks et al. 2013). The experiment is certainly affected by wood species properties. In fact, softwood (i.e., wood that lacks vessels and multi-seriate rays) behaves in a more uniform way than hardwood (Boonstra et al. 2006a, b) because its great vessels and parenchymatic rays are prone to damage during the preparatory stage. These dimensions of the vessels and multi-seriate rays change not only due to cell wall contraction, but also because of the shrinkage of the surrounding, more densely packed tissue (i.e., fibers or tracheids; Boonstra et al. 2006b).

In the current observations, the three-dimensional organization of the cellular wood structure withstands the high tension and deformations resulting from the continuous increase of T without generating fractures or cracks ex novo (Figs. 3, 5).

However, previous small fractures in the wall surface are amplified, sometimes in a very intensive way, during heat treatment; amplifications beyond 300 % were observed (Fig. 6).

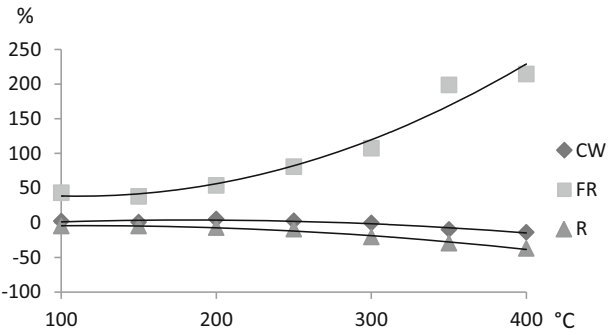

Fig. 6 Dimensional (%) divergence between fractures (FR), cell wall (CW), and parenchymatic rays (R) during heating

Small deformations that occur during the preparation and cutting of the specimen, such as the partial detachment of the middle lamella (similar to Biziks et al. 2013) or traces left by the last row of parenchymatic rays cells, are sufficient to generate samples that are entirely crossed by cracks and fractures by the end of the experiment (Figs. 3, 6).

In conclusion, the use of ESEM demonstrates great potential for investigating wood reactions to heat treatment. For each type of analyzed element, the cell wall thickness was clearly nonlinear during heating, which was valid for each type of analyzed element. Future research studies should involve new methods of measurements (e.g., by pixel, gray tones image analysis) and other variables (e.g., time or pressure, different wood species).

References

Adewopo JB, Patterson DW (2011) Effects of heat treatment on the mechanical properties of Loblolly pine, Sweetgum, and Red Oak. For Prod J 61(7):526–535

Awoyemi L, Jones IP (2011) Anatomical explanations for the changes in properties of western red cedar (Thuja plicata) wood during heat treatment. Wood Sci Technol 45(2):261–267

Biziks V, Andersons B, Beļkova Ļ, Kapača E, Militz H (2013) Changes in the microstructure of birch wood after hydrothermal treatment. Wood Sci Technol 47(4):717–735

Blechschmidt J, Engert P, Stephan M (1986) The glass transition of wood from the viewpoint of mechanical pulping. Wood Sci Technol 20(3):263–272

Boonstra MJ, Rijsdijk JF, Sander C, Kegel E, Tjeerdsma B, Militz H, van Acker J, Stevens M (2006a) Microstructural and physical aspects of heat treated wood. Part 1. Softwoods. Maderas Cienc Tecnol 8(3):193–208

Boonstra MJ, Rijsdijk JF, Sander C, Kegel E, Tjeerdsma B, Militz H, van Acker J, Stevens M (2006b) Microstructural and physical aspects of heat treated wood. Part 2. Hardwoods. Maderas Cienc Tecnol 8(3):209–217

Bourgois J, Guyonnet R (1988) Characterization and analysis of torrefied wood. Wood Sci Technol 22(2):143–155

Bryne LE, Lausmaa J, Ernstsson M, Englund F, Walinder MEP (2010) Ageing of modified wood. Part 2: determination of surface composition of acetylated, furfurylated, and thermally modified wood by XPS and ToF-SIMS. Holzforschung 64(3):305–313

Davis WH, Thompson WS (1964) Influence of thermal treatments of short duration on the toughness and chemical composition of wood. For Prod J 14(3):50–356

Esteves BM, Pereira HM (2009) Wood modification by heat treatment: a review. BioResources 4(1):370–404

Fengel D, Wegener G (1989) Wood: chemistry, ultrastructure, reactions. Walter de Gruyter, Berlin

Giebeler E (1983) Dimensional stabilization of wood by moisture-heat-pressure treatment. Holz Roh-Werkst 41(1):87–94

Kamdem DP, Pizzi A, Jermannaud A (2002) Durability of heat-treated wood. Holz Roh- Werkst 60(1):1–6

Kubojima Y, Okano T, Ohta M (2000) Bending strength and toughness of heat-treated wood. J Wood Sci 46(1):8–15

Mitsui K (2006) Changes in colour of spruce by repetitive treatment of light irradiation and heat treatment. Holz Roh- Werkst 64:243–244

Pelaez-Samaniegoa MR, Yadamac V, Garcia-Pereza M, Lowelle E, McDonald AG (2014) Effect of temperature during wood torrefaction on the formation of lignin liquid intermediates. J Anal Appl Pyrolysis 109:222–233

Sehlstedt-Persson M, Johansson D, Morén T (2006) Effect of heat treatment on the microstructure of pine, spruce and birch and the influence on capillary absorption. In: Proceedings of the 5th IUFRO

symposium "wood structure and properties'06", Sliač—Sielnica, Slovakia, Sept 3–6 2006, pp 251–255
Turkulin H, Holzer L, Richter K, Sell J (2005a) Application of the ESEM technique in wood research: part I. Optimization of imaging parameters and working conditions. Wood Fiber Sci 37(4):552–564
Turkulin H, Holzer L, Richter K, Sell J (2005b) Application of the ESEM technique in wood research. Part II. Comparison of operational modes. Wood Fiber Sci 37(4):565–573
Xie Y, Liu Y, Sun Y (2002) Heat-treated wood and its development in Europe. J For Res 13(3):224–230